Journal of Molecular Liquids 288 (2019) 111055

Contents lists available at ScienceDirect

Journal of Molecular Liquids

journal homepage: www.elsevier.com/locate/molliq

# Theoretical studies on racemization of levetiracetam: Structural movements, character of hydroxide ion and guidelines for efficient control

Zhen Li [a,1], Chengjun Wu [a,1], Jiazu Liu [a], Linwei Li [a], Changshan Sun [b,*], Tiemin Sun [a,*]

[a] Key Laboratory of Structure-Based Drug Design and Discovery, Shenyang Pharmaceutical University, Ministry of Education, Shenyang 110016, PR China
[b] Pharmacy Department, Shenyang Pharmaceutical University, Shenyang 110016, PR China

ARTICLE INFO

*Article history:*
Received 16 March 2019
Received in revised form 5 May 2019
Accepted 26 May 2019
Available online 30 May 2019

*Keywords:*
Levetiracetam
Racemization mechanism
Density functional theory

ABSTRACT

Levetiracetam, a novel antiepileptic drug, is administered as the *S*-enantiomer of etiracetam according to the predominant pharmacodynamic advantage compared to its *R*-enantiomer. Thus, the content of enantiomer is restricted explicitly, which creates a hotspot focused on the stereochemistry of levetiracetam during synthesis. However, unexpected racemization was observed during our practice. It's important to understand the racemization mechanism for levetiracetam. In this article, the racemization process for levetiracetam is comprehensively explored by means of widely used density functional theory. Firstly, basic structural movements were determined for further description of racemization process. Then, five plausible pathways for isolated levetiracetam were identified with detailed elucidation of structural movements during racemization. Significant energy barriers were observed corresponding to the proton transfer process, which demonstrated the chiral stability of levetiracetam in neutral environment. Further, hydroxide ion was introduced to elucidate the character of it in racemization process. The result indicated that hydroxide ion could facilitate the racemization by dramatically reducing the barriers for proton transfer, which was further confirmed by the experiment. Additionally, several suggestions were proposed according to the theoretical mechanism and experimental observation, resulting in the efficient control of racemization extent during synthesis. Finally, qualified levetiracetam could be prepared in kg-scale.



## 1. Introduction

Chirality is commonly found in launched and developing drugs [1–3]. Since the organism is constructed by chiral substrates, chiral amino acids for example, it could take different responses to the drugs with different chirality. The different stereochemistry of drug may lead to enormous contrast in pharmacodynamics and pharmacokinetics. When one enantiomer declaims main action for therapeutics, the other enantiomer may be inactive, reveals less medical potency, even has antagonistic effect against the active one or be responsible for the side effect when taking racemate [1,4]. Hence, several chiral drugs, which are previously administered as racemic, have been replaced with the most active stereoisomer recently. And the preference for single enantiomer is increasing when a new drug are under development or approaching to the market [3,5,6].

Levetiracetam, (*S*)-α-ethyl-2-oxo-pyrrolidine acetamide, is practiced as a novel broad-spectrum antiepileptic drug for both adult and paediatric patients clinically [7]. It has been administered as the *S*-enantiomer of etiracetam due to the superior pharmacodynamic advantage compared to the *R*-enantiomer [8]. Consequently, in order to eliminate the burden caused by impotent enantiomer, the limitation of its *R*-enantiomer is explicitly stipulated, which establishes a hotspot focused on maintaining stereochemistry or developing asymmetric synthetic strategy during synthesis [9–11]. Previously in our internal practice, an improved one-pot method was performed for preparation of levetiracetam according to the reported method [12,13], starting with commercialized (*S*)-2-aminobutanamide hydrochloride and 4-chlorobutyryl chloride. However, excessive enantiomer was observed in final product (more than 9.11%). In this method, levetiracetam was prepared from qualified chiral source, suggesting an unexpected racemization process taken place plausibly during synthesis. Nevertheless, this synthetic method we performed is preferred in the industrialized preparation of levetiracetam due to its convenience and conciseness. Moreover, this strategy is also involved as intermediate steps in other reported methods which are proceeded in similar reaction conditions [14,15]. Therefore, the racemization and the solution for reducing racemization should be highly regarded during synthesis, leading to the requirement for process optimization. As a matter of fact, the

* Corresponding authors.
*E-mail addresses:* freescs@163.com (C. Sun), suntiemin@126.com (T. Sun).
[1] These authors contributed equally to this work.

https://doi.org/10.1016/j.molliq.2019.111055
0167-7322/

investigation of reaction mechanism could provide valuable information about structural and electrical properties, which is conducive to understand structural movements in the reaction process and provide guidelines for reaction optimization. Hence, the mystery of racemization could be decrypted with the help of thorough understanding of racemization mechanism and chiral stability of levetiracetam. However, no racemization mechanism for levetiracetam has been presented so far.

Benefitted from the development of computational chemistry, various reaction mechanisms could be precisely simulated to give special insights for estimating the practicability of reaction [16–18]. In this article, the racemization mechanism for levetiracetam is firstly illustrated by theoretical calculation. Density functional theory (DFT) [19], a widely utilized method for simulating reaction mechanism, was implemented to elucidate the racemization process of levetiracetam. Firstly, basic structural movements were determined in order to describe the racemization process on continuous potential energy surface. Then, the racemization for isolated levetiracetam was carried out as fundamental mechanism to understand the structural movements during racemization process. Further, according to the observation of racemization in base condition, hydroxide ion was introduced to understand the character of it in racemization. Moreover, frontier molecular orbitals (FMOs) were carried out to describe the transfer of electron density in complex structure during racemization [20]. Additionally, the importance of hydroxide ion was further characterized by kinetic experiment. Subsequently, the influence factors for racemization were elucidated according to the theoretical mechanism and experimental observation. The racemization was efficiently controlled after modifying the synthetic procedure based on the suggestions. The aim of this article is not only to establish the theoretical models in racemization process for levetiracetam in isolated form and associated with hydroxide ion, but also provide guidelines for reducing racemization in synthesis of levetiracetam and its derivatives.

## 2. Materials and methods

### 2.1. Computational method

Firstly, conformational distribution analysis for levetiracetam and its *R*-enantiomer was conducted by Spartan 14 program using molecular mechanics force field (MMFF94) [21,22]. Considerable conformers for each enantiomer were obtained within 10 kJ $mol^{-1}$. These conformers were further optimized using Gaussian 09 program package [23]. DFT method, especially the Becke 3–Lee–Yang–Parr (B3LYP) exchange-correlation functional [19,24], is commonly implemented for elucidating structural properties and reaction mechanism. Thus, the structural optimization was performed at B3LYP/6-311 G (d, p) level. And the geometries of transition states were obtained by means of the Synchronous Transit-guided Quasi-Newton (STQN) method. The thermodynamics parameters were obtained by vibrational frequencies calculation which was conducted at the same level. The nature of corresponding stationary points (minima or transition state) was confirmed according to the number of imaginary frequency (0 or 1). Furthermore, the intrinsic reaction coordinate (IRC) path was performed to verify that the transition states connect to the reactant and product of the proposed mechanism [25]. Additionally, for the consideration of solvent effect, polarized continuum model (PCM) method was utilized with the assignment of dichloromethane as solvent [26].

### 2.2. Preparation of levetiracetam

(*S*)-2-aminobutanamide hydrochloride (30.0 g) was mixed with dichloromethane (300 mL), and tetra-butyl ammonium bromide (3.5 g) was added. Then, the reaction mixture was cooled to −15 °C. The further addition of potassium hydroxide and 4-chlorobutyryl chloride was divided into three batches. For each round, potassium hydroxide (20.2 g) was added first with vigorous stirring for 10 min. After that, the solution of 4-chlorobutyryl chloride (12.2 g) in dichloromethane (45 mL) was slowly added to maintain the temperature under −10 °C. The reaction was stirred vigorously at −10 °C for further 45 min before adding another batch of potassium hydroxide and 4-chlorobutyryl chloride. After adding total three batches, the reaction mixture was stirred at −10 °C for over 2 h. Additional potassium hydroxide (6.6 g) was added into the reaction mixture followed by stirring for 4 h. Then, the insoluble substance was filtered and washed by dichloromethane (10 × 3 mL). The organic layer was combined and neutralized by acetic acid. The unwanted salt was filtered and washed by dichloromethane (10 × 3 mL). The combined organic layer was dried by anhydrous sodium sulfate and then filtered. Dichloromethane was evaporated under reduced pressure followed by the addition of ethyl acetate (150 mL). The solution was concentrated to over 75 mL to afford slurry. The slurry was stirred at −5 °C for an hour. The precipitate was filtered and washed by cold ethyl acetate (10 × 3 mL), and then dried under a vacuum at 30 °C to give 27.5 g of crude product. The crude product was recrystallized in isopropanol (40 mL) to afford refined product of levetiracetam as white solid (22.3 g, yield 60.5%). purity: 99.67%; *ee*: 99.94%; *m.p.*: 116.0 °C–118.0 °C; $[\alpha]_D^{25}$: −90.0° (*c* = 1, EtOH); HRESIMS *m/z*: 193.0948 [M Na] (*calcd.* for $C_8H_{14}O_2N_2Na$, 193.0947); $^1$H NMR (600 MHz, $CDCl_3$): δ 6.98 (s, 1H), 6.61 (s, 1H), 4.52 (t, *J* = 5 Hz, 1H), 3.51–3.55 (m, 1H), 3.37–3.41 (m, 1H), 2.43 (t, *J* = 8.5 Hz, 2H), 2.02–2.07 (m, 2H), 1.93–1.98 (m, 1H), 1.65–1.70 (m, 1H), 0.89 (t, *J* = 7.5 Hz, 3H); $^{13}$C NMR ($CDCl_3$, 150 MHz): δ 175.7, 172.6, 55.5, 43.4, 30.7, 21.0, 17.8, 10.2; ECD revealed a negative cotton effect at around 223 nm, which was consisted with reported ECD behavior of levetiracetam.

## 3. Results and discussion

### 3.1. Analysis of basic structural movements in racemization process

In order to facilitate the description, the 2D structure of levetiracetam is presented in Fig. 1 with selected atoms numbered. Reaction process could be described as the continuous movements on potential energy surface. Therefore, it's important to determine the structural movements which are essential in elucidating the process. In this case, the most stable conformer for levetiracetam and its *R*-enantiomer was obtained as the initial and final structure in the racemization process, shown in Fig. 2 (conformer S1 and R1). The racemization process from S1 to R1 requires two kinds of structural movements: 1) the proton H19 should transfer from one side of chiral carbon C7 to the other, which refers to a proton abstraction followed by a readdition process; and 2) the conformational isomerization should occur to achieve the stable conformer of the other enantiomer after racemization.

#### 3.1.1. Proton transfer

The proton from chiral center transferring from one side to the other is crucial process in the chiral conversion, which usually associates with breaking and reforming of C—H bond. As the first step, breaking of chemical bond requires massive energy, resulting in a relatively unstable system. In order to stabilize the system after proton leaving, an

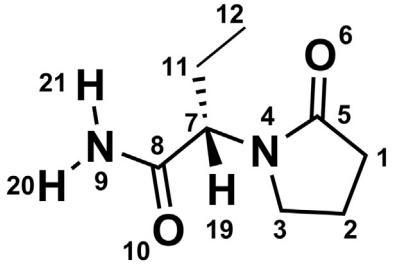


**Fig. 1.** 2D structure of levetiracetam with numbers of selected atoms.

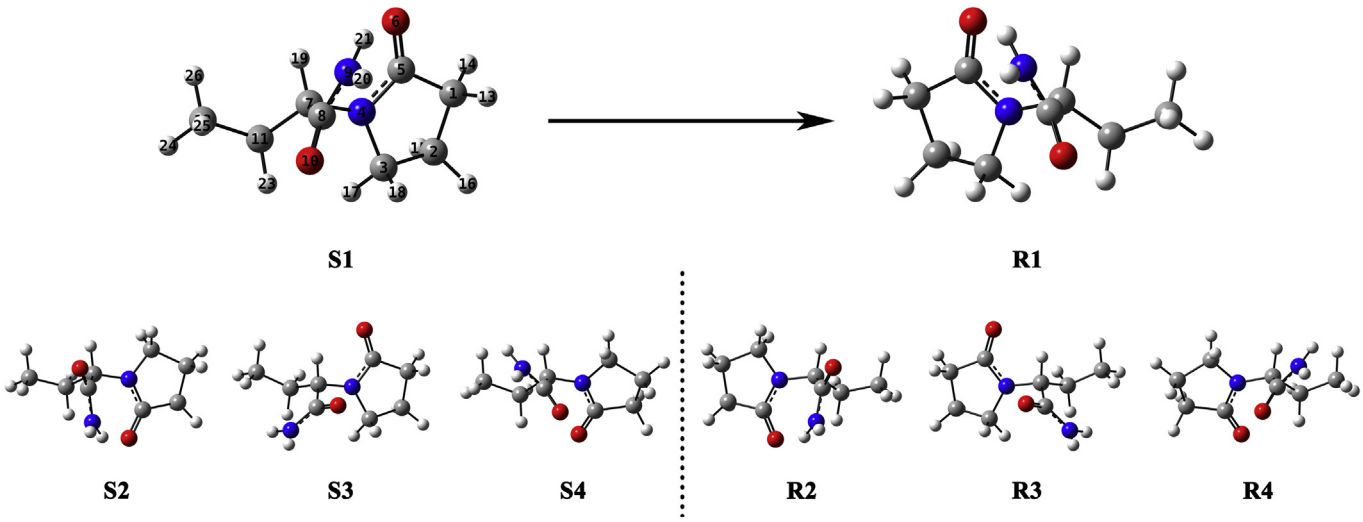


**Fig. 2.** Conformers of levetiracetam and its *R*-enantiomer involving in the racemization pathways.

acceptor with high electron density is needed to seize the electropositive proton. Furthermore, in order to accomplish chiral conversion, the proton should return to the carbon at the other side. Therefore, an appropriate proton acceptor is required to not only seize the proton during abstraction, but also transferring the proton to the other side like a carrier.

*3.1.2. Conformational isomerization*

The chiral conversion is a continuous process, which could not be fully understood without appropriate conformational changes. Moreover, the different conformations could reveal the different steric hindrance and electrical properties around reactive site, leading to the difference on reactive potential. And, it has been indicated that the conformational changes play an important role in racemization process [27]. Therefore, the investigation of conformational isomerization is conducive to understand the conformation effect during mechanism simulation.

The conformational changes usually associate with rotation of single bonds and ring torsion. In this case, during the isomerization from S1 to R1, the ethyl, amide and pyrrolidone moieties should rotate nearly 180° through the rotation of corresponding single bonds adjacent to chiral center. And the torsion of pyrrolidone ring could be accomplished by flipping the C2 from one side of pyrrolidone ring to the other. Apparently, it is complex and exhausting to consider all four types of conformational changes along with proton transfer process. To simplify the process, it's essential to determine the type of changes that has more important influence on the conformational stability. Then, relaxed scan calculation was carried out as preliminary evidence to evaluate the energy barrier of conformational change and the influence on conformational stability. The result of energy change was shown in Supporting information.

The torsion scan of pyrrolidone ring was performed by rotating the dihedral angle of C2—C3—N4—C5 from −22.66° to 27.34°. A stationary point is found when the dihedral rotated to 11.34°. Compared to initial conformer, only a little higher total energy (0.40 kcal $mol^{-1}$) is observed, which indicates the torsion of pyrrolidone ring has no significant impact on the stability of whole molecule. The energy barrier of torsion is 0.88 kcal $mol^{-1}$, suggesting this type of conformation change is easy to accomplish.

The rotation scan of ethyl group is represented by the angle change of N4—C7—C11—C12. The highest energy barrier is 7.38 kcal $mol^{-1}$ and a stationary point is observed after rotating over −130° from the original position. The total energy of this conformer is found 4.94 kcal $mol^{-1}$ higher than initial conformer.

For amide group, the relative energy is continuously increasing with the change of dihedral angle O10—C8—C7—N4 from −99.89° to 130.11°, indicating the rotation of amide group is adverse to the conformational stability. The decrease of conformational stability is attributed to the breaking of intramolecular hydrogen bond formed between N9—H21 from amide and C5═O6 from pyrrolidone ring, which demonstrates that this hydrogen bond has unnegligible influence on conformational stability. And an indistinctive stationary point was obtained after rotating over 160° from the original position with the increased total energy of 6.87 kcal $mol^{-1}$. Based on these, the rotation of amide group has great correlation to the conformational stability. Moreover, the rotation of amide group is further found as a critical premise for proton transfer process of isolated levetiracetam, which will be discussed later in this article.

The rotation scan of pyrrolidone ring is performed by the rotation of dihedral angle C5—N4—C7—C8, whereas the highest energy barrier (9.88 kcal $mol^{-1}$) is found higher than other types of conformational changes. And it's observed that the amide group is significantly rotated along with the rotation of pyrrolidone ring during the scan calculation. Such behavior indicates that the rotation of pyrrolidone ring is plausibly hindered and the subsequent rotation of relative flexible amide group could lower the tension. This explanation could be supported by the rotation scan of pyrrolidone ring with additional freezing the rotation of amide group, whereas the total energy is continuously increasing without rotation of amide group. Moreover, a sudden decrease of total energy is observed when the dihedral angle changes from 150° to 160°. According to the corresponding structures, the sudden change is plausibly attributed to the reformation of hydrogen bond between amide (N9—H21) and carbonyl (C5═O6) on the different side from the original position. Based on these, the relative position between pyrrolidone and amide moiety has strong impact on the stability of conformation, which should be taken into account in the conformational isomerization process.

*3.2. Mechanism for racemization of isolated levetiracetam*

Fundamentally, in order to understand the structural movements during racemization process, the mechanism is primarily elucidated in the simplest situation by using the isolated levetiracetam as theoretical model.

*3.2.1. Proposal of racemization pathways*

For isolated levetiracetam, the vicinal carbonyl group (C8═O10) from amide group could be regarded as an appropriate acceptor to

capture reactive proton, leading to the formation of an enol-like intermediate. Similar conversion is often found in the racemization process of amino acids [28–30]. Therefore, it's plausible to propose that a keto-enol tautomerization takes place during racemization. In the structure of conformer S1, the vicinal carbonyl is located at the *anti*-position of C—H with the distance of 3.23 Å, which is adverse for proton transfer. In order to facilitate proton transfer, the vicinal carbonyl is better to be positioned at the same side with C7-H19 (*syn*-position), which could decrease the distance between H19 and O10. Therefore, the appropriate rotation of amide group is required before proton abstraction.

In the summary of structural movements, proton transfer should take place twice at least during racemization, corresponding to the proton abstraction and readdition respectively. And for conformational isomerization, it has been demonstrated that an appropriate rotation of amide is necessary before proton abstraction. According to previous discussion, the rotation of pyrrolidone ring also should be considered, which could take place between any aforementioned steps. Therefore, five plausible racemization pathways for isolated levetiracetam are depicted in Fig. 3. In pathway **a** (S1 → S4 → S2 → Enol1 → R3 → R1) and **b** (S1 → S3 → S2 → Enol1 → R3 → R1), the rotation of pyrrolidone ring takes place before the proton abstraction. The difference between these two pathways is the rotation of pyrrolidone ring occurring before or after the required rotation of amide group. In pathway **c** (S1 → S3 → Enol2 → Enol3 → R3 → R1), the rotation of pyrrolidone ring take place between the proton abstraction and readdition process. In pathway **d** (S1 → S3 → Enol2 → R2 → R3 → R1) and **e** (S1 → S3 → Enol2 → R2 → R4 → R1), the rotation of pyrrolidone ring occurs after proton readdition. And the difference between these two pathways is also attributed to the ring rotation occurring before or after the rotation of amide group. The structural movements in pathway **a** are described in following discussion. The details of the rest pathways are depicted in Supporting information. And the structures of intermediates and transition states are illustrated in Fig. 4, whereas the corresponding geometrical and thermodynamics parameters are listed in Table 1.

*3.2.2. Study of structural movements in pathway **a***

In step 1, the pyrrolidone ring of S1 rotates first with the change of dihedral angle C5—N4—C7—C8 ($\alpha$) from −83.63° to 98.72°, leading to the generation of S4 via the transition state TS1. And moderate change of the dihedral angle O10—C8—C7—N4 ($\beta$) (from −99.89° to −34.04°) is observed corresponding to the rotation of amide group, which also has been demonstrated in scan calculation. The vibrational mode of imaginary frequency of TS1 confirms rotating potential of amide group during the ring rotation. The energy barrier of this change is 10.44 kcal mol$^{-1}$, which is similar to the energy barrier observed in scan calculation. Such energy barrier is mostly attributed to the breaking of hydrogen bond between amide (N9—H21) and carbonyl (C5═O6). The free energy of S4 is 7.31 kcal mol$^{-1}$ higher than S1 comparatively, which also suggests the formation of hydrogen bond is the main reason causing the stabilization of conformation.

Step 2 involves the rotation of amide group, corresponding to the isomerization from S4 to S2 via TS2. The rotating tendency of amide is verified by the vibrational mode of imaginary frequency of TS2. The angle $\beta$ changes to 118.77° with slight change of pyrrolidone ring (from 98.72° to 74.93°). In the structure of S2, the hydrogen bond is reformed at the other side, resulting in the decreased relative energy from 7.31 kcal mol$^{-1}$ (S4) to 1.39 kcal mol$^{-1}$ (S2). The energy barrier of this step is 1.23 kcal mol$^{-1}$, indicating that the rotation of amide is easy to accomplish after ring rotation. More importantly, after amide rotation, the carbonyl C8═O10 from amide group rotates to the same side with C7—H19, leading to decreasing the distance (2.42 Å) between O10 and H19. With the more appropriate angle of C7—H19—O10 (76.31°), the proton transfer could take place on S2 more easily than initial conformer S1.

In step 3, proton abstraction occurs causing the structure change from the *S*-enantiomer (S2) to the achiral enol-like intermediate (Enol1). In the structure of transition state TS3, the proton H19 transfer from C7 to O10 from vicinal carbonyl, which is confirmed by the imaginary frequency. During the proton transfer, the extra negative charge from C7 is delocalized via the resonance between carbon and vicinal amide group, resulting in a conjugated system and establishing the achiral planar structure. The angle $\beta$ notably changes from 118.77° to −2.77° associated with moderate change of angle $\alpha$ from 74.93° to 55.90°. In order to conduct this step, a significant barrier of 59.39 kcal mol$^{-1}$ should be overcome, which is mainly caused by breaking chemical bond. And compared to initial structure, this intermediate Enol1 is

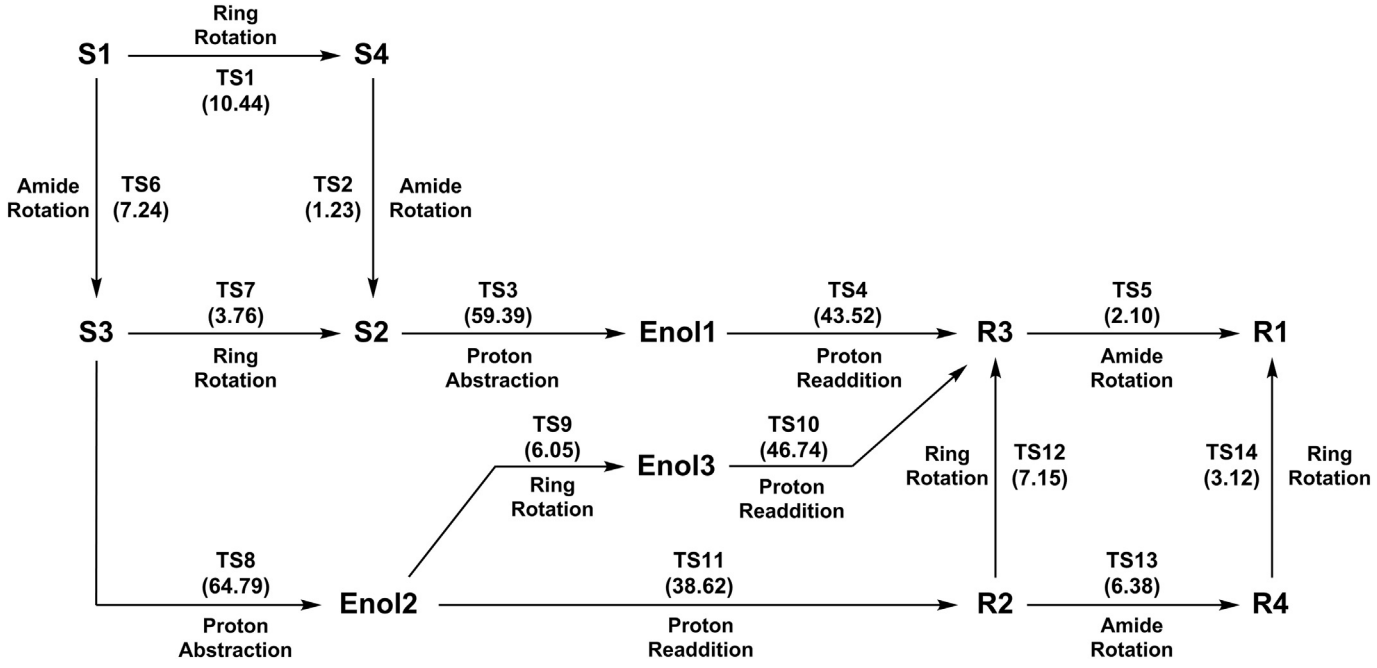


**Fig. 3.** Plausible racemization pathways for isolated levetiracetam with corresponding Gibbs free energy barriers of each step at 298 K (in kcal mol$^{-1}$, shown in brackets).

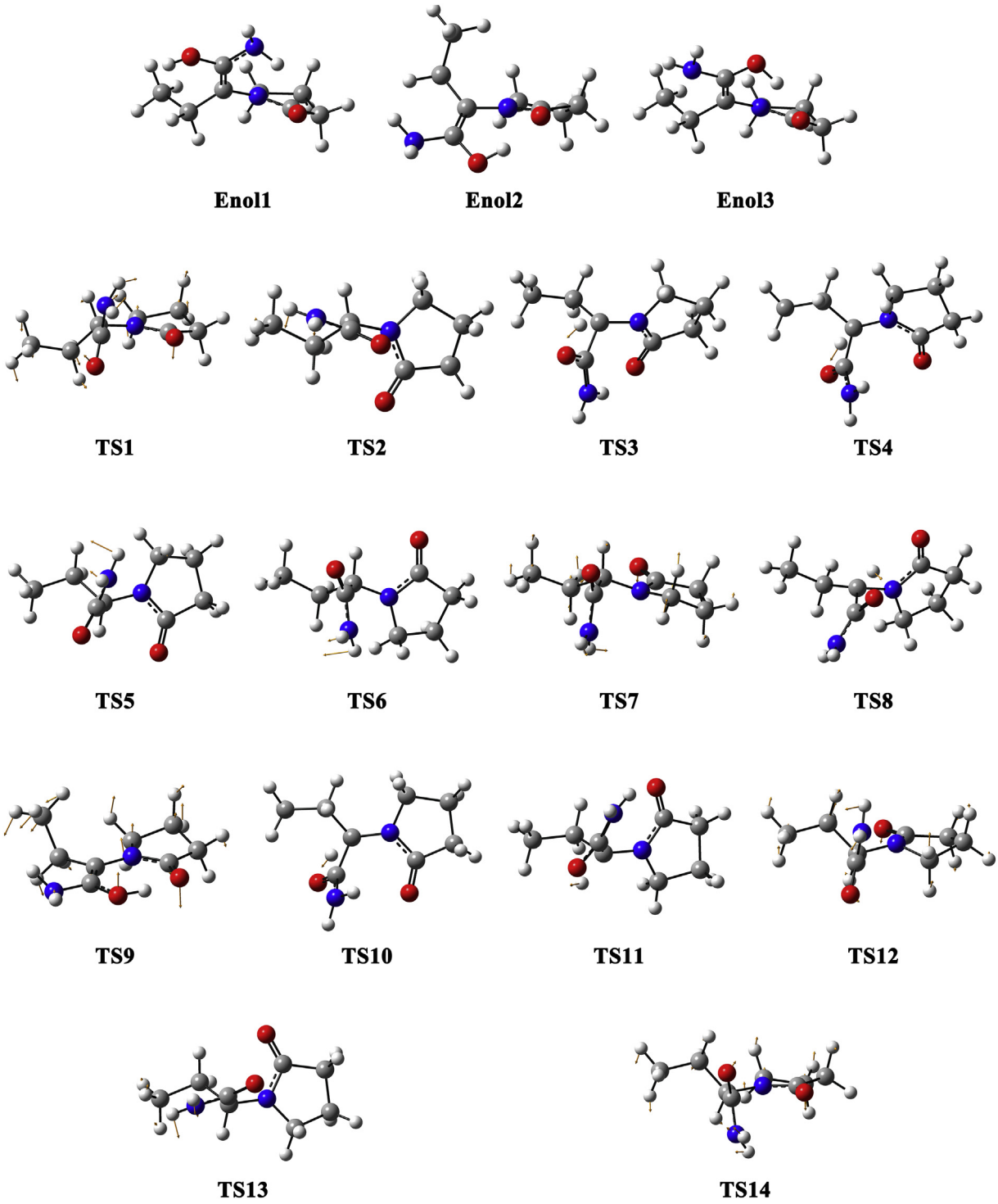


**Fig. 4.** Optimized structures of intermediates and transition states involving in the racemization mechanism for isolated levetiracetam.

relatively unstable with high energy (25.45 kcal $mol^{-1}$ higher than S1), suggesting this structure is reactive and easy to conduct further conversion.

Step 4 involves the proton readdition from O10 to C7 through different track against step 3, leading to the formation of *R*-enantiomer. In this step, the proton turns to the other side of the carbon with the help of appropriate rotation of amide group, which is confirmed by the change of angle $\beta$ changes from −2.77° (Enol1) to −139.88° (TS4). The energy barrier of this step is 43.52 kcal $mol^{-1}$. After that, the established conformer (R3) of *R*-enantiomer is relatively unstable compared to R1, which requires further conformational isomerization.

In step 5, an additional rotation of amide group takes place, resulting in the conformational change from R3 to most stable conformer R1. The dihedral angle $\beta$ changes from −56.31° to 99.89° accompanied with moderate change of angle $\alpha$ from 120.76° to 83.63°. The rotation needs to overcome a small barrier of 2.10 kcal $mol^{-1}$.

### 3.2.3. Comparison of structural movements in pathways

According to previous analysis, appropriate rotation of amide group is required before proton abstraction. In pathway **a** and **b**, the rotation of pyrrolidone ring also occurs before proton abstraction. Based on the energy barriers in these two pathways, the rotation of amide is more

**Table 1**
Geometric parameters and corresponding relative energies of the structures involving in the racemization mechanism for isolated levetiracetam.

| | D1[a] | D2[a] | $\theta$[b] | $\alpha$[c] | $\beta$[c] | $\Delta E_{ZPE}$[d] | $\Delta G$[e] |
|---|---|---|---|---|---|---|---|
| S1 | 1.09 | 3.23 | 36.46 | −83.63 | −99.89 | 0.00 | 0.00 |
| S2 | 1.09 | 2.42 | 76.31 | 74.93 | 118.77 | 1.51 | 1.39 |
| S3 | 1.10 | 2.67 | 64.49 | −118.36 | 51.26 | 6.03 | 4.78 |
| S4 | 1.10 | 3.23 | 36.25 | 98.72 | −34.04 | 8.38 | 7.31 |
| Enol1 | 2.46 | 0.96 | 74.71 | 55.90 | −2.77 | 25.30 | 25.45 |
| Enol2 | 2.51 | 0.99 | 71.95 | −47.95 | 4.51 | 21.83 | 22.11 |
| Enol3 | 2.52 | 0.99 | 71.74 | 46.88 | −4.44 | 21.95 | 22.35 |
| R1 | 1.09 | 3.23 | 36.46 | 83.63 | 99.89 | 0.00 | 0.00 |
| R2 | 1.09 | 2.42 | 76.28 | −75.05 | −119.03 | 1.47 | 1.34 |
| R3 | 1.10 | 2.64 | 65.90 | 120.76 | −56.31 | 6.11 | 5.24 |
| R4 | 1.10 | 3.24 | 35.84 | −99.03 | 35.65 | 8.39 | 7.29 |
| TS1 | 1.10 | 3.21 | 36.84 | −3.94 | −96.41 | 9.41 | 10.44 |
| TS2 | 1.10 | 3.09 | 44.78 | 81.88 | −5.07 | 8.38 | 8.54 |
| TS3 | 1.59 | 1.19 | 106.02 | 58.33 | 136.75 | 60.51 | 60.78 |
| TS4 | 1.58 | 1.21 | 105.67 | 52.87 | −139.88 | 69.14 | 68.97 |
| TS5 | 1.09 | 2.46 | 74.77 | 101.38 | −129.22 | 7.22 | 7.34 |
| TS6 | 1.09 | 2.46 | 74.77 | −101.19 | 129.61 | 7.20 | 7.24 |
| TS7 | 1.10 | 2.46 | 74.68 | 179.78 | 113.28 | 7.86 | 8.54 |
| TS8 | 1.57 | 1.24 | 104.88 | −97.05 | 76.02 | 69.91 | 69.57 |
| TS9 | 2.55 | 1.00 | 72.76 | 5.67 | −4.15 | 26.63 | 28.17 |
| TS10 | 1.62 | 1.18 | 104.68 | 31.09 | −137.09 | 69.50 | 69.09 |
| TS11 | 1.59 | 1.19 | 106.02 | −58.43 | −136.69 | 60.49 | 60.73 |
| TS12 | 1.10 | 2.46 | 74.66 | 178.42 | −111.60 | 7.85 | 8.49 |
| TS13 | 1.10 | 3.10 | 44.02 | −75.51 | 6.91 | 7.29 | 7.72 |
| TS14 | 1.10 | 3.21 | 36.89 | 3.22 | 96.65 | 9.39 | 10.40 |

[a] D1 and D2 denotes the distance of C7···H19 and O10···H19 in Å respectively.
[b] $\theta$ denotes the angle of C7—H19—O10 in degrees.
[c] $\alpha$ and $\beta$ denotes the dihedral angle of C5—N4—C7—C8 and O10—C8—C7—N4 in degrees respectively.
[d] $\Delta E_{ZPE}$ represents the relative energy including the zero-point energy (ZPE) correlation in kcal mol$^{-1}$.
[e] $\Delta G$ represents the relative Gibbs free energy at 298 K in kcal mol$^{-1}$.

favorable than rotating pyrrolidone ring at first. Furthermore, after rotation of amide, the energy barrier of rotating pyrrolidone ring is reduced due to the potential of reforming the hydrogen bond between N9—H21 and C5═O6. As a consequence, conformer S2 is generated with a little higher energy compared to S1.

In pathway **a** and **b**, the proton abstraction could take place on conformer S2 due to the reduced distance between O10 and H19 (2.42 Å). The corresponding energy barrier is 59.39 kcal mol$^{-1}$. For the rest of pathways, rotation of pyrrolidone ring takes place after proton abstraction, resulting in the proton abstraction taking place on conformer S3. The distance between O10 and H19 is 2.67 Å in conformer S3, which could be responsible for the higher energy barrier (64.79 kcal mol$^{-1}$) for proton abstraction than S2.

After the proton abstraction, the achiral planar structure Enol1 and Enol2 is established respectively due to the electronic delocalization through resonance effect. And in pathway **c**, the rotation of pyrrolidone ring occurs on Enol2, which leads to the formation of Enol3. All three enol-like structures are relatively unstable compared to initial structure, suggesting these structures are reactive and easy to conduct further conversion.

The proton could approach to the other side of the carbon with the help of appropriate rotation of amide group. And the proton transfers from O10 to C7 through different track against the abstraction process to complete the chiral conversion. The energy barrier of this step is around 40 kcal mol$^{-1}$. And after proton readdition, the structure could change to the most stable conformer R1 with appropriate rotation of amide group in pathway **a**, **b** and **c**, while the rotation of pyrrolidone ring occurs after chiral conversion in pathway **d** and **f**. And due to the steric hindrance, the rotation of amide group is preferred to occur at first in these two pathways.

In summary, the highest energy barrier is attributed to the proton transfer from C7 to O10, corresponding to the conversion from *S*-enantiomer to enol-like intermediate. Such high energy barrier suggests that levetiracetam is relatively stable in neutral condition. This result is consistent with the experimental reports that the chiral conversion of levetiracetam is difficult to take place in solid state and even in vivo environment [31]. Comparing the energy barriers of all pathways, it is revealed that a conformational preference occurring on S2 (59.39 kcal mol$^{-1}$) than S3 (64.79 kcal mol$^{-1}$) during proton abstraction. Therefore, this theoretical model not only indicates the chiral stability of levetiracetam, but also demonstrating different capacity of proton transfer on different conformers and providing detailed structural movements which is helpful for further exploration of mechanism.

### 3.3. Mechanism for hydroxide ion catalyzed racemization of levetiracetam

In the previous discussion, the racemization of isolated levetiracetam is restricted by the high energy barriers attributed to the proton transfer between C7 and O10. However, unnegligible excess of *R*-enantiomer was observed by the chiral HPLC analysis, indicating the racemization of levetiracetam occurred indeed during synthetic process. When reviewing the procedure, the use of potassium hydroxide draws our attention. And it has been demonstrated that base-catalyzed racemization is common among amino acids [30]. During the synthesis, potassium hydroxide is assigned with multiple missions including neutralization of (*S*)-2-aminobutanamide hydrochloride and free acid generated during acylation and cyclization. As the outcome, water is generated after the neutralization, which could facilitate the ionization of potassium hydroxide. The hydroxide ion provided by potassium hydroxide could replace the carbonyl from amide acting as a proton carrier during proton transfer. And the process of proton abstraction from C7 could be accelerated due to the strong negative electricity of hydroxide ion. Therefore, hydroxide ion is introduced to understand the character of it in the racemization of levetiracetam.

Since the proton carrier is replaced by the hydroxide ion, the premise, rotation of amide group before proton abstraction in the isolated levetiracetam, is no longer required in the hydroxide ion catalyzed racemization process. Therefore, the hydroxide ion could be directly interacted with the most stable conformer (S1). And according to previous investigation, the difference of energy barriers for proton transfer has been observed on different conformers. Hence, other stable conformer (S2) is also investigated. Based on these, two racemization pathways are carried out starting with the complex structure formed by hydroxide ion interacting with conformer S1 and S2 respectively. The optimized complex structures are illustrated in Figs. 5 and 7 respectively, whereas the introduced hydroxide ion is numbered as O27 and H28. And the corresponding geometrical and thermodynamics parameters are presented in Table 2.

#### 3.3.1. Pathway ***A***: $OH^-\cdot S1 \rightarrow H_2O\cdot SC^-1 \rightarrow H_2O\cdot RC^-1 \rightarrow OH^-\cdot R2$

In the structure of $OH^-\cdot S1$, there is an additional hydrogen bond established between the hydrogen H28 from $OH^-$ and the carbonyl O6═C5 from pyrrolidone ring, which locates the $OH^-$ right on the top of chiral center. The distance (D2) between oxygen O27 from $OH^-$ and proton H19 from chiral center is 2.94 Å. In step 1, the proton H19 transfers from C7 to O27, which is demonstrated by the increased distance of D1 and decreased distance of D2 in transition state TS′1. This proton transfer potential is also verified by the vibration mode of imaginary frequency of TS′1. The energy barrier for proton abstraction is calculated as 4.87 kcal mol$^{-1}$, which is much lower than that in isolated levetiracetam (≈60 kcal mol$^{-1}$). It suggests that hydroxide ion could facilitate the proton abstraction by significantly reducing the energy barrier. The complex structure of a carbanion and water molecule ($H_2O\cdot SC^-1$) is established after proton abstraction. The dihedral angle $\beta$ changes to 167.14°, indicating the formation of conjugated planar structure. The extra electron is delocalized via the resonance between carbanion and vicinal amide group. The relative free energy of complex $H_2O\cdot SC^-1$ is obtained as 3.19 kcal mol$^{-1}$ lower than initial complex $OH^-\cdot S1$.

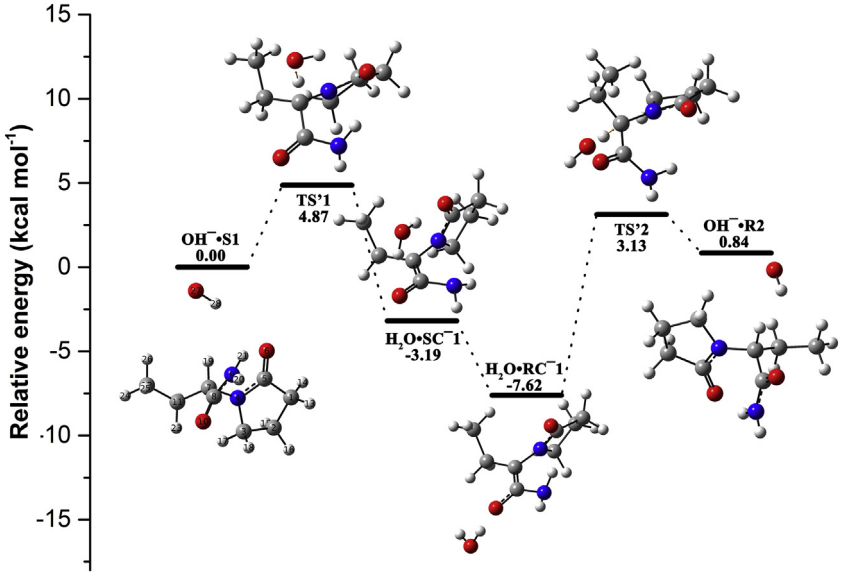


**Fig. 5.** Optimized structures and corresponding relative Gibbs free energies at 298 K (in kcal mol$^{-1}$) involving in the hydroxide ion catalyzed racemization pathway **A**.

Therefore, the proton abstraction associated by hydroxide ion is an exothermic process and could take place easily.

In order to reverse configuration, the proton from water molecule should be re-seized by carbanion from the other side of conjugated plane. Therefore, water migration is required to turn the proton to the other side, corresponding to the conformational change from complex $H_2O \cdot SC^-1$ to $H_2O \cdot RC^-1$. After migration, the relative free energy of complex structure changes to −7.62 kcal mol$^{-1}$, which is probably attributed to the formation of two hydrogen bonds in $H_2O \cdot RC^-1$ (O6···H21—N9 and O10···H28—O27) rather than one in $H_2O \cdot SC^-1$ (O6···H28—O27). After that, the proton returns to C7 at the different side from the proton abstraction via transition state TS′2. And the proton readdition needs to overcome an energy barrier of 10.75 kcal mol$^{-1}$, which is higher than the barrier of proton abstraction. After the proton readdition, the conformation of *R*-enantiomer is formed with the geometrical parameters close to R2. Therefore, appropriate conformational isomerization is necessary for converting conformer R2 to R1 stepwise, which is previously described in the racemization of isolated levetiracetam. The highest energy barrier of conformational isomerization is predicted as 6.43 kcal mol$^{-1}$, which is unnegligible compared to the energy barrier of proton transfer.

The highest occupied molecular orbital (HOMO) represents the electron that has the highest potential to delocalize in the reaction [20]. The HOMOs of the complex structures in this pathway are illustrated in Fig. 6. In the HOMO of complex $OH^- \cdot S1$, the electron is mostly localized on the O27 from hydroxide ion, indicating the potential of electron transfer is correlated to the reactivity of hydroxide ion. And after the proton abstraction, the electron density relocates on the carbanion and also vicinal groups, which verifies that the stabilization of carbanion structure is attributed to the electronic delocalization through the resonance with vicinal groups. Combined the electron distribution in the HOMO of all complex involved in this pathway, the electron transfer tendency could be clearly described with the orientation opposite to the proton transfer.

**Table 2**
Geometric parameters and corresponding relative energies of the structures involving in the hydroxide ion catalyzed racemization mechanism.

| | D1[a] | D2[a] | $\theta$[b] | $\alpha$[c] | $\beta$[c] | $\Delta E_{ZPE}$[d] | $\Delta G$[e] |
|---|---|---|---|---|---|---|---|
| $OH^- \cdot S1$ | 1.09 | 2.94 | 171.92 | −84.98 | −96.62 | 0.00 | 0.00 |
| $OH^- \cdot S2$ | 1.09 | 2.48 | 173.76 | 74.18 | 123.60 | 0.20 | 0.57 |
| $OH^- \cdot R1$ | 1.09 | 3.00 | 169.28 | 85.98 | 96.14 | 0.13 | 0.50 |
| $OH^- \cdot R2$ | 1.09 | 2.59 | 169.52 | −74.65 | −123.56 | 0.28 | 0.84 |
| $H_2O \cdot SC^-1$ | 3.00 | 0.98 | 111.03 | −70.46 | 167.14 | −4.53 | −3.19 |
| $H_2O \cdot SC^-2$ | 3.88 | 0.96 | 92.19 | 59.27 | 174.38 | −7.04 | −7.07 |
| $H_2O \cdot RC^-1$ | 4.01 | 0.96 | 85.57 | −58.90 | −174.67 | −7.14 | −7.62 |
| $H_2O \cdot RC^-2$ | 2.99 | 0.97 | 111.69 | 70.38 | −168.38 | −5.28 | −4.19 |
| TS′1 | 1.33 | 1.32 | 176.82 | −79.97 | −148.22 | 2.78 | 4.87 |
| TS′2 | 1.36 | 1.28 | 175.62 | −54.57 | 160.27 | 2.01 | 3.13 |
| TS′3 | 1.36 | 1.28 | 175.38 | 54.70 | −160.82 | 2.18 | 3.43 |
| TS′4 | 1.33 | 1.32 | 176.53 | 79.14 | 148.29 | 2.83 | 4.71 |

[a] D1 and D2 denotes the distance of C7···H19 and O27···H19 in Å respectively.
[b] $\theta$ denotes the angle of C7—H19—O27 in degrees.
[c] $\alpha$ and $\beta$ denotes the dihedral angle of C5—N4—C7—C8 and O10—C8—C7—N4 in degrees respectively.
[d] $\Delta E_{ZPE}$ represents the relative energy including the zero-point energy (ZPE) correlation in kcal mol$^{-1}$.
[e] $\Delta G$ represents the relative Gibbs free energy at 298 K in kcal mol$^{-1}$.

### 3.3.2. Pathway **B**: $OH^- \cdot S2 \rightarrow H_2O \cdot SC^-2 \rightarrow H_2O \cdot RC^-2 \rightarrow OH^- \cdot R1$

In this pathway, the initial complex is formed by hydroxide ion interacted with conformer S2 (shown in Fig. 7). The conformational isomerization from S1 to S2 is discussed before in pathway **a** and **b** with the appropriate rotation of amide and pyrrolidone ring, and the highest energy barrier is 10.44 kcal mol$^{-1}$. Since the carbonyl of amide is close to C7—H19 in S2, the carbonyl C9═O10 could replace the carbonyl C5═O6 from pyrrolidone ring in S1 to establish a hydrogen bond with $OH^-$. As a result, the $OH^-$ is placed on the top of C7-H19 to form the complex structure $OH^- \cdot S2$. The distance D2 is obtained as 2.48 Å after optimization, suggesting the formation of more intimate complex and stronger potential for proton abstraction compared to $OH^- \cdot S1$ (D2 = 2.94 Å). The proton abstraction is conducted via transition state TS′3. The vibrational mode of imaginary frequency describes the proton transfer between C7 and O28. And the formation of planar carbanion is revealed by the change of angle $\beta$ from 123.60° to 174.38°. The energy barrier for proton abstraction is predicted as 2.86 kcal mol$^{-1}$, which is even lower than that in pathway **A**. This result also verified that a more intimate complex is formed between $OH^-$ and S2, which further facilitate the proton abstraction.

As pathway **A**, water migration should also take place before proton readdition in this pathway, leading to the conformational change from $H_2O \cdot SC^-2$ to $H_2O \cdot RC^-2$. Then, the proton H19 is re-seized by carbanion C7 through the transition state TS′4, resulting in the formation of *R*-enantiomer. The conformation of formed *R*-enantiomer shows similar

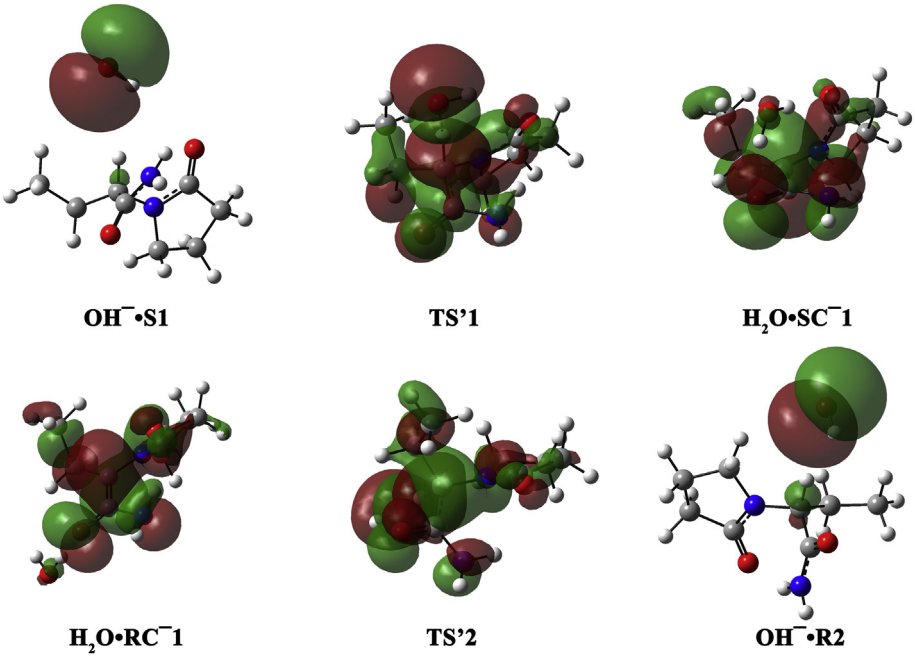


**Fig. 6.** The HOMO of corresponding structures involving in the hydroxide ion catalyzed racemization pathway **A**.

geometrical parameters (shown in Table 2) to conformer R1. And the energy barrier of proton readdition is calculated as 8.90 kcal mol$^{-1}$.

Additionally, the HOMOs of these structures reveal the similar electron transfer potential in this pathway referred to pathway **A**, which has been shown in Fig. 8.

These two pathways demonstrate that the proton transfer, which is the most difficult process for isolated levetiracetam, could be efficiently facilitated by hydroxide ion with significantly reducing the energy barrier. The highest energy barrier is predicted as 10.75 kcal mol$^{-1}$ and 8.90 kcal mol$^{-1}$ respectively in pathway **A** and **B**, suggesting the racemization of levetiracetam could take place easily under base condition. And pathway **B** is little more favorable than pathway **A** because of the relative lower barriers for both proton abstraction and readdition process. It indicates that the conformational isomerization from S1 to S2 is favorable for the $OH^-$ catalyzed racemization.

### *3.4. Studies of influence factors for racemization*

Previously, theoretical study demonstrates the catalysis of hydroxide ion in the racemization process. Then, the kinetics study is carried out to evaluate the racemization rate of levetiracetam experimentally (shown in Supporting information). Dichloromethane and potassium hydroxide, which are used in synthetic procedure, is utilized as solvent and base to create an experimental environment approximated to synthesis process. The result reveals the racemization of levetiracetam proceeds rapidly at room temperature. The rate constant is determined as 0.00034 s$^{-1}$ and the energy barrier is calculated as 20.09 kcal mol$^{-1}$. The experimental barrier is close to the theoretical barrier found in hydroxide ion catalyzed mechanism, compared to that in racemization for isolated levetiracetam. The deviation is plausibly attributed to the incomplete ionization of potassium hydroxide in apolar solvent, whereas

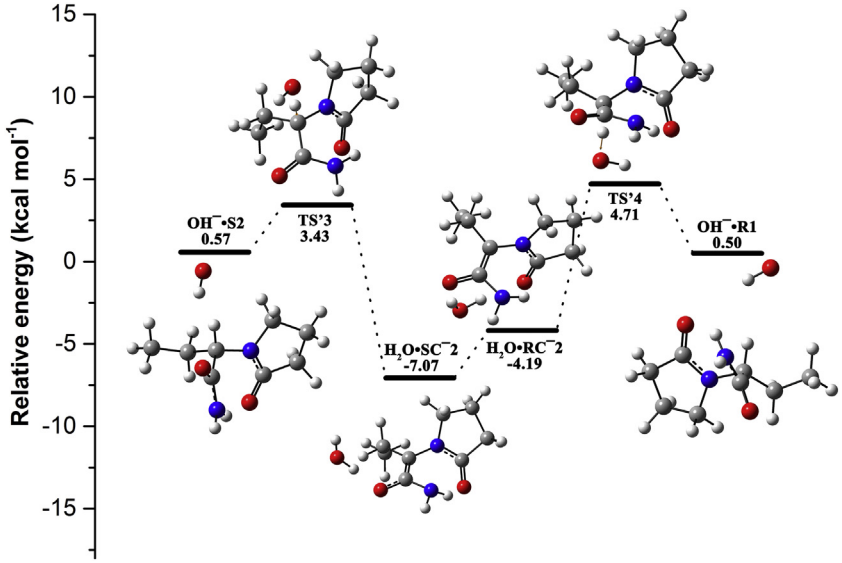


**Fig. 7.** Optimized structures and corresponding relative Gibbs free energies at 298 K (in kcal mol$^{-1}$) involving in the hydroxide ion catalyzed racemization pathway **B**.

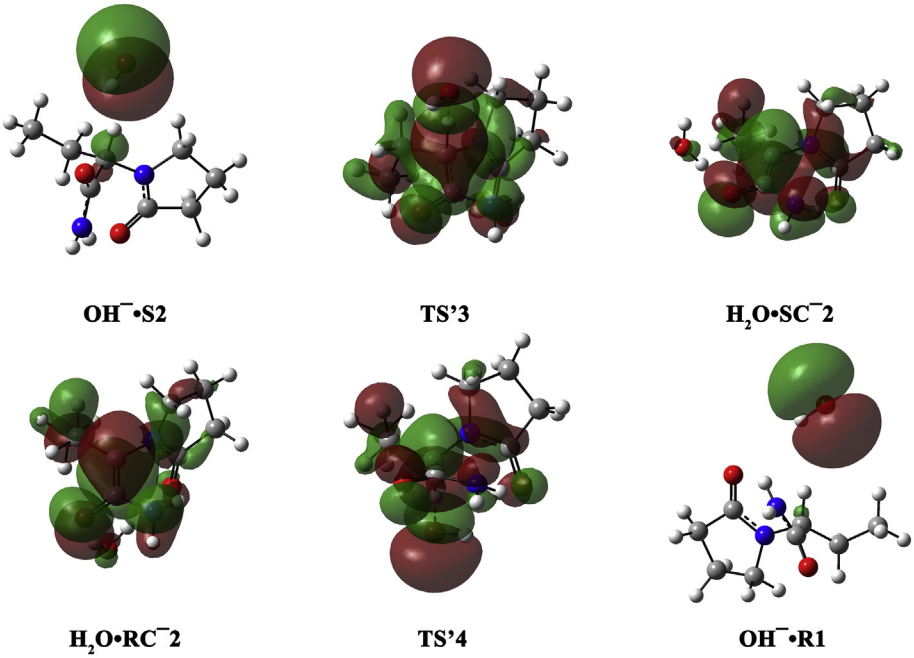


**Fig. 8.** The HOMO of corresponding structures involving in the hydroxide ion catalyzed racemization pathway **B**.

the theoretical calculation is based on the completely ionized hydroxide ion.

In control experiment, optically pure levetiracetam is dissolved in the potassium hydroxide absented dichloromethane, whereas the racemization is not observed (shown in Supporting information). This result verifies the theoretical investigation that levetiracetam is optically stable in neutral condition. However, potassium hydroxide is assigned for multiple missions including neutralization of (*S*)-2-aminobutanamide hydrochloride and free acid generated during acylation and cyclization. Therefore, the use of potassium hydroxide is critical for proceeding reaction. It has been revealed that the racemization rate is correlated to pH of the solution [32,33], corresponding to the content of potassium hydroxide in this case. Although the utilization of base is ineluctable, the addition of potassium hydroxide could be divided in several batches. As a consequence, the content of base could be controlled in a relative lower level, which could reduce the racemization.

Except the use of base, it has been demonstrated that temperature has significant influence on rate constant in base catalyzed racemization [33]. Therefore, the extent of racemization is estimated in five different temperatures. As a result, the rate of racemization is slowed down remarkably when temperature is below zero (shown in Supporting information). Thus, lowering temperature is a feasible option for reaction optimization.

Then, according to the suggestions, the addition of potassium hydroxide and 4-chlorobutyryl chloride is divided into three batches and the reaction temperature is controlled under −10 °C. As a result, the racemization extent is controlled in 0.03%, whereas the synthesis process of levetiracetam still proceeds smoothly. Further, qualified levetiracetam was prepared in kg-scale using the modified procedure (shown in Supporting information).

## 4. Conclusion

In this article, DFT method was implemented to illustrate the mechanism for racemization of levetiracetam and characterize the importance of hydroxide ion during the chiral conversion. Firstly, two kinds of basic structural movements were determined, corresponding to the proton transfer and conformational isomerization process. Then, the racemization for isolated levetiracetam was carried out as fundamental mechanism, whereas five plausible pathways were proposed with detailed structural movements. Two significant energy barriers were found in each pathway, corresponding to the proton abstraction (≈60 kcal $mol^{-1}$) and readdition (≈40 kcal $mol^{-1}$) process. Such high barriers indicated levetiracetam is relative stable in neutral condition, which agreed with reported stereochemical stability profile of levetiracetam. Further, we demonstrated hydroxide ion could accelerate the racemization process by acting as a proton carrier in proton transfer, leading to the dramatically reduction of the energy barrier. The highest barrier was found around 10 kcal $mol^{-1}$ during the proton readdition. Additionally, the experimental barrier was obtained as 20.09 kcal $mol^{-1}$ by kinetic study, which was approximate to the theoretical barrier found in hydroxide ion associated racemization. The effect of content of hydroxide and temperature was elucidated according to the theoretical mechanism and experimental observation, which also provided guidelines for control of racemization during synthesis. After adding potassium hydroxide in three batches and carefully controlling temperature under −10 °C, the racemization was efficiently reduced. After appropriate modification of the synthetic procedure, kg-scale levetiracetam could be prepared in good quality.

## Appendix A. Supplementary data

Supplementary data to this article can be found online at https://doi.org/10.1016/j.molliq.2019.111055.

## References

[1] H. Caner, E. Groner, L. Levy, I. Agranat, Trends in the development of chiral drugs, Drug Discov. Today 9 (2004) 105–110.
[2] W.H. Brooks, W.C. Guida, K.G. Daniel, The significance of chirality in drug design and development, Curr. Top. Med. Chem. 11 (2011) 760–770.
[3] A. Calcaterra, I. D'Acquarica, The market of chiral drugs: chiral switches versus de novo enantiomerically pure compounds, J. Pharm. Biomed. 147 (2017) 323–340.
[4] B. Testa, Chiral aspects of drug metabolism, Trends Pharmacol. Sci. 7 (1986) 60–64.
[5] A. Israel, C. Hava, C. John, Putting chirality to work: the strategy of chiral switches, Nat. Rev. Drug Discov. 1 (2002) 753–768.
[6] I. Agranat, S.R. Wainschtein, The strategy of enantiomer patents of drugs, Drug Discov. Today 15 (2010) 163–170.
[7] K.A. Lyseng Williamson, Levetiracetam: a review of its use in epilepsy, Drugs 71 (2011) 489–514.

[8] M. Noyer, M. Gillard, A. Matagne, J.P. Hénichart, E. Wülfert, The novel antiepileptic drug levetiracetam (ucb L059) appears to act via a specific binding site in CNS membranes, Eur. J. Pharmacol. 286 (1995) 137.
[9] S.P. Kotkar, A. Sudalai, A short enantioselective synthesis of the antiepileptic agent, levetiracetam based on proline-catalyzed asymmetric α-aminooxylation, Tetrahedron Lett. 47 (2006) 6813–6815.
[10] R. Mylavarapu, R.V. Anand, L.A. Reddy, G.S. Reddy, A. Roy, A. Bhattacharya, K. Mukkanti, R. Bandichhor, An alternate synthesis of levetiracetam, Green Chem. Lett. Rev. 3 (2010) 225–230.
[11] K.D. Sarma, Z. Ji, H. Yun, J.G. Davidson, Amino acid esters and amides for reductive amination of mucochloric acid: synthesis of novel γ-lactams, short peptides and antiseizure agent levetiracetam (Keppra®), Eur. J. Org. Chem. 2010 (2006) 3730–3737.
[12] A.K. Mandal, S.W. Mahajan, P. Ganguly, A. Chetia, N.D. Chauhan, N.D. Bhatt, R.R. Baria, Process for Preparing Levetiracetam and Racemization of (*R*)-and (*S*)-2-amino Butynamide and the Corresponding Acid Derivatives, US 2008/0194840 A1, August 14 2008.
[13] P.V. Acharyulu, C.H. Raju, Preparation of amino acid amides, US 2005/0182262 A1, August 18, 2005.
[14] A.K. Mandal, S.W. Mahajan, M.K. Sharma, A. Chetia, N.D. Chauhan, Process for Preparing Levetiracetam, US 2008/0146819 A1, June 19 2008.
[15] M. Kandula, Compositions and methods for the treatment of epilepsy, US 9, 290, 486 B1, March 22, 2016.
[16] M.D. Bhatt, J.Y. Lee, Oxygen reduction reaction (ORR) kinetics through different solvents of the non-aqueous electrolyte in Li-air (O2) batteries in both the gas and solution phases: a DFT study, J. Mol. Liq. 271 (2018) 274–280.
[17] I. Tankov, R. Yankova, Quantum mechanical and reaction dynamics investigation of butyl acetate synthesis in the presence of pyridinium hydrogen sulfate, J. Mol. Liq. 278 (2019) 183–194.
[18] I. Tankov, R. Yankova, DFT analysis, reaction kinetics and mechanism of esterification using pyridinium nitrate as a green catalyst, J. Mol. Liq. 277 (2019) 241–253.
[19] A.D. Becke, Density-functional thermochemistry. III. The role of exact exchange, J. Chem. Phys. 98 (1993) 5648–5652.
[20] C.G. Zhan, J.A. Nichols, D.A. Dixon, Ionization potential, electron affinity, electronegativity, hardness, and electron excitation energy: molecular properties from density functional theory orbital energies, J. Phys. Chem. A 107 (2003) 4184–4195.
[21] Y. Shao, L.F. Molnar, Y. Jung, J. Kussmann, C. Ochsenfeld, S.T. Brown, A.T. Gilbert, L.V. Slipchenko, S.V. Levchenko, D.P. O'Neill, Advances in methods and algorithms in a modern quantum chemistry program package, Phys. Chem. Chem. Phys. 8 (2006) 3172–3191.
[22] T.A. Halgren, Merck molecular force field. I. Basis, form, scope, parameterization, and performance of MMFF94, J. Comput. Chem. 17 (1996) 490–519.
[23] M. Frisch, G. Trucks, H.B. Schlegel, G.E. Scuseria, M.A. Robb, J.R. Cheeseman, G. Scalmani, V. Barone, B. Mennucci, G. Petersson, Gaussian 09, Revision A. 02, 200, Gaussian, Inc., Wallingford, CT, 2009.
[24] A.D. Becke, Density-functional exchange-energy approximation with correct asymptotic behavior, Phys. Rev. A 38 (1988) 3098–3100.
[25] K. Fukui, The path of chemical reactions—the IRC approach, Acc. Chem. Res. 14 (1981) 471–476.
[26] G. Scalmani, M.J. Frisch, Continuous surface charge polarizable continuum models of solvation. I. General formalism, J. Chem. Phys. 132 (2010) 2027–2081.
[27] C. Tian, P. Xiu, Y. Meng, W. Zhao, Z. Wang, R. Zhou, Enantiomerization mechanism of thalidomide and the role of water and hydroxide ions, Chem. Eur. J. 18 (2012) 14305–14313.
[28] A. Neuberger, Stereochemistry of amino acids, Adv. Protein Chem. 4 (1948) 297–383.
[29] O. Takahashi, K. Kobayashi, A. Oda, Computational insight into the mechanism of serine residue racemization, Chem. Biodivers. 7 (2010) 1625–1629.
[30] P. D'Arrigo, D. Arosio, L. Cerioli, D. Moscatelli, S. Servi, F. Viani, D. Tessaro, Base catalyzed racemization of amino acid derivatives, Tetrahedron Asymmetry 22 (2011) 851–856.
[31] N. Isoherranen, B. Yagen, S. Soback, M. Roeder, V. Schurig, M. Bialer, Pharmacokinetics of levetiracetam and its enantiomer (*R*)-α-ethyl-2-oxo-pyrrolidine acetamide in dogs, Epilepsia 42 (2001) 825–830.
[32] J.S. Kim, Y.S. Lee, Effect of reaction pH on enolization and racemization reactions of glucose and fructose on heating with amino acid enantiomers and formation of melanoidins as result of the Maillard reaction, Food Chem. 108 (2008) 582–592.
[33] A.C. Cabordery, M. Toussaint, N. Azaroual, J.P. Bonte, P. Melnyk, C. Vaccher, C. Foulon, Kinetics and mechanism of racemization of Tic-hydantoins, potent sigma-1 agonists, Tetrahedron Asymmetry 22 (2011) 125–133.